

Article

Structural Features and Thermal Behavior of Ion-Exchanged Clinoptilolite from Beli Plast Deposit (Bulgaria)

Louiza Dimowa^{1,*}, Nadia Petrova¹, Yana Tzvetanova¹ , Ognyan Petrov¹ and Iskra Piroeva²

¹ Institute of Mineralogy and Crystallography, Bulgarian Academy of Sciences, Acad. Georgi Bonchev Str., Bl. 107, 1113 Sofia, Bulgaria

² Institute of Physical Chemistry, Bulgarian Academy of Sciences, Acad. Georgi Bonchev Str., Bl. 11, 1113 Sofia, Bulgaria

* Correspondence: louiza.dimova@gmail.com

Abstract: The structural features and the thermal behavior of natural, Na-, Ca-, K-, Mg-, and Cd-exchanged clinoptilolite from the Beli Plast deposit (Bulgaria) were studied. Purified clinoptilolite sample was preliminary prepared and ion-exchanged at 100 °C for six days. DSC-TG analyses were performed for all studied forms. The effects in the DSC curves show differences with temperature due to release of weakly bound H₂O molecules and strongly bound ones. The endotherm minima temperatures were between 78 and 115 °C decreasing in the sequence K- < Na- < Natural- < Ca- ≤ Mg- < Cd-clinoptilolite. The hydrate complexes around the exchanged cations also influenced the DSC curves. The cation-coordinating H₂O molecules and the non-coordinating ones were determined by XRD structural refinement for all exchanged samples. The H₂O molecules of the cation-hydrate complexes are released at higher temperatures than weakly bound ones and affected the DSC curves differently. The structural adjustments made by the Rietveld method, as well as the applied EDS analyzes for the chemical composition of the samples, allowed us to correlate these data to the thermal characteristics of the studied clinoptilolite samples.



Citation: Dimowa, L.; Petrova, N.; Tzvetanova, Y.; Petrov, O.; Piroeva, I. Structural Features and Thermal Behavior of Ion-Exchanged Clinoptilolite from Beli Plast Deposit (Bulgaria). *Minerals* **2022**, *12*, 1576. <https://doi.org/10.3390/min12121576>

Academic Editor: Rossella Arletti

Received: 11 November 2022

Accepted: 7 December 2022

Published: 8 December 2022

Publisher's Note: MDPI stays neutral with regard to jurisdictional claims in published maps and institutional affiliations.



Copyright: © 2022 by the authors. Licensee MDPI, Basel, Switzerland. This article is an open access article distributed under the terms and conditions of the Creative Commons Attribution (CC BY) license (<https://creativecommons.org/licenses/by/4.0/>).

Keywords: clinoptilolite; ion exchange; Rietveld refinement; DSC-TG(DTG)

1. Introduction

Clinoptilolite is defined as the zeolite mineral series with HEU-type framework topology and Si/Al ratio > 4 [1,2]. The structure-type code HEU is allocated by the Structure Commission of the International Zeolite Association (IZA) and listed in Meier et al. [3]. Minerals with the same framework topology but with Si/Al < 4.0 are classified as heulandite mineral series, with which clinoptilolite forms a continuous series. Clinoptilolite has monoclinic symmetry and the space group *C2/m* is the maximum symmetry which may be lowered to *C2* or *Cm* [2,4]. The HEU-type topology is characterized by a sheetlike organization of the aluminosilicate framework into layers perpendicular to the *b* axis [5,6]. There is a two-dimensional system of three types of channels defined by ten- and eight-membered tetrahedral rings. The large ten-membered A channel and the smaller eight-membered B channel are parallel to the *c* axis and both intersect the eight-membered C channel, which is parallel to the *a* axis [7,8]. The channels are occupied by exchangeable cations (mainly Na⁺, K⁺, and Ca²⁺), which are coordinated by H₂O molecules in irregular polyhedra and/or by framework oxygens [9]. Mg²⁺, Ba²⁺, and Sr²⁺ are, in some cases, substantial. Fe²⁺ and Fe³⁺ are also possible constituents. The charge balance is achieved by variable Si–Al substitution in the tetrahedral framework.

Four extra-framework cation positions are recognized in the tetrahedral framework of the HEU-type zeolite: M(1), M(2), M(3), and M(4). Ca²⁺ and Na⁺ cations are located at M(1) and M(2) positions; M(1) tends to accommodate more Na than M(2). The position M(3) is specific for K and is located almost at the center of the eight-membered ring of the channel

parallel to a axis. Mg^{2+} is located at M(4) position, which is octahedrally coordinated by six H_2O molecules [8,10,11].

The behavior of zeolites at high temperatures is a very important characteristic that is used in various fields of material sciences ranging from their industrial application to their identification. Numerous zeolites are used as molecular sieves, in gas adsorption, in drying of gases, as selective catalysts, in a high-level radioactive waste repository, etc. and the understanding of their thermal behavior and appropriate activation temperatures is crucial [12]. The thermal behavior has also been suggested as a method to distinguish between similar zeolites, such as clinoptilolite and heulandite [13]. In addition, the zeolite content in mixtures or in zeolitic tuffs can be determined through the H_2O desorption behavior. Detailed studies of the structural effects accompanying hydration/dehydration processes permit evaluation of the conditions that lead to structural modification or breakdown [12].

A large number of studies report on the properties of natural zeolites and their ion-exchanged forms after thermal treatments [1,13–15] or on the dehydration behavior and polymorphism of heulandite-group zeolites [1,16–18]. In a thermal study, Knowlton et al. [19] distinguished three types of water associated with clinoptilolite—external water, loosely bound zeolitic water, and tightly bound zeolitic water, at 75°, 171°, and 271 °C, respectively. Investigations of the thermal behavior and thermal transformation properties of natural clinoptilolites and their cation-exchanged forms allows us to obtain information for possible technological applications [20–24]. The thermal behavior of the clinoptilolite/heulandite minerals has most often been studied by considering the changes in the intensity of the 020 diffraction peak after heating [1,13,25–29]. Koyama and Takeuchi [8] suggested that the occupancy of K^+ at M(3) position in clinoptilolite structure is one of the controlling factors of the thermal behavior of the heulandite-group zeolites. K-rich clinoptilolites tend to be thermally stable through high-temperature structural studies [28,30,31].

The Si/Al ratio, the specific position of the extra-framework cations within the structure, their coordination by H_2O molecules, and interactions with framework oxygens also influence the thermal behavior of the clinoptilolite [6,8–10,12,32–34].

Single crystal structure refinements of clinoptilolite showed variations in extra-framework cation sites compared with heulandite as a function of the extent of dehydration [5,10,35]. Cappelletti et al. [11] examined two natural clinoptilolites with different chemical composition using TG-DTG-DTA analysis and Rietveld refinement based on synchrotron data to define cationic populations of the exchangeable cation sites. They concluded that the Mg(4) position, if occupied by Mg^{2+} , gives only a partial contribution to the exchange, whereas the Mg^{2+} present in the other sites can be more easily removed.

The aim of the present study was to follow in more detail the dehydration specificity of natural clinoptilolite from the Beli Plast deposit (Bulgaria) and its Na-, K-, Ca-, Mg-, and Cd-exchanged forms. Comparative investigations were performed using Rietveld-based powder X-ray diffraction structural analysis and differential scanning calorimetry and thermogravimetry in order to elucidate the manner of dehydration of the non-coordinating H_2O molecules in the pores (loosely bound H_2O molecules) and tightly bound H_2O molecules forming the close coordination spheres in relation to specific structural cation- H_2O configurations.

2. Materials and Methods

The studied material is a zeolitized tuff from the volcanogenic sedimentary deposit Beli Plast related to Early Oligocene acid volcanism (Eastern Rhodopes, Bulgaria) [36–38]. The mineral composition of the tuff is: ~80% clinoptilolite associated with feldspars, montmorillonite, illite, celadonite, calcite, and opal-CT. The associated minerals in the studied sample were removed by heavy liquid separation and treatment with a NaOH solution for removal of opal-C [39], yielding almost pure clinoptilolite (cpt) designated as Natural-cpt in the study, with structural formula $Na_{1.01}Ca_{1.76}K_{1.11}Mg_{0.49}Al_{6.29}Si_{29.61}O_{72}21.05 H_2O$ (Table 1).

Table 1. Chemical composition (EDS, wt%) and structural formula of clinoptilolite based on 72 O atoms.

Samples Oxides	Purified Natural-cpt	Na-cpt	K-cpt	Ca-cpt	Mg-cpt	Cd-cpt
SiO ₂	66.21	66.91	66.47	66.03	65.32	62.07
Al ₂ O ₃	11.94	12.05	12.11	11.81	11.91	11.18
MgO	0.74	0.49	0.49	0.43	2.76	0.30
CaO	3.68	0.66	0.51	5.20	1.81	1.19
Na ₂ O	1.16	5.48	0.24	0.38	0.27	0.24
K ₂ O	1.94	0.59	8.70	0.34	0.96	0.64
CdO	–	–	–	–	–	9.1
Fe ₂ O ₃	0.21	0.17	0.15	0.16	0.17	0.18
H ₂ O	13.8	13.3	11.0	15.5	16.6	14.9
Σ	99.68	99.65	99.67	99.85	99.80	99.80
Atoms per formula unit (apfu)						
Si	29.61	29.66	29.62	29.73	29.59	29.65
Al	6.29	6.29	6.36	6.27	6.37	6.29
Mg	0.49	0.32	0.33	0.29	1.87	0.21
Ca	1.76	0.31	0.24	2.51	0.88	0.61
Na	1.01	4.71	0.21	0.33	0.24	0.22
K	1.11	0.33	4.95	0.20	0.56	0.39
Cd	–	–	–	–	–	2.03
Fe	0.04	0.10	0.05	0.05	0.06	0.06
H ₂ O	21.05	20.19	16.83	23.49	25.40	24.02

Ion exchange procedures were performed at 100 °C in 1 M solutions of Na, K, Ca, Mg, and Cd nitrates (Sigma-Aldrich Chemie GmbH, Taufkirchen, Germany) for 6 days. The solutions (20 mL) and the Natural-cpt sample (0.4 g) were placed in Teflon autoclaves. The autoclaves were shaken several times per day and the solutions were renewed two times. Before renewal pH values were checked and the values were >4.7–4.9. The ion-exchanged samples were filtered, washed with distilled water, and dried at room temperature. The obtained ion-exchanged forms were labelled as Na-, K-, Ca-, Mg-, and Cd-cpt.

Powder X-ray diffraction (PXRD) patterns were collected at room temperature on a PANalytical EMPYREAN Diffractometer system with a goniometer radius of 240 mm, operating at 40 kV and 30 mA, theta–theta geometry, with CuK α radiation, equipped with 3D-pixel detector. PXRD measurements were recorded in Bragg–Brentano geometry from 3 to 100° in 2theta with a scanning rate of 0.013°/80 s. Standard sample holders with 0.5 mm depth were used. The Rietveld method [40] was applied for structural refinement of all samples. The atomic coordinates and occupancy of extra-framework cations were refined using the Bruker AXS Topas v. 4.0 suite of programs [41]. The refinements of the studied clinoptilolite forms were conducted with the structural model of Koyama & Takeuchi [8] at room temperature.

SEM EDS analyses were performed on a JSM 6390 electron microscope (Japan) in conjunction with energy dispersive X-ray spectroscopy (EDS, Oxford INCA Energy 350, HighWycombe, Buckinghamshire, UK) equipped with ultrahigh resolution scanning system (ASID-3D) at the following conditions: 20 kV accelerating voltage, I ~ 75 mA, vacuum medium in the range of 10^{−4} Pa, spot size 1 μ m. The powders of the clinoptilolite forms were pressed into pellets and coated with carbon to determine chemical composition with SEM-EDS, using appropriate standards. The reported concentrations for each sample are average values from the ten measurements carried out on the pellet.

Thermal analyses: Differential scanning calorimetry (DSC) and thermogravimetry (TG) were carried out on apparatus SETSYS2400 Evolution, SETARAM at the following conditions: temperature range from 20 to 700 °C in a static air atmosphere with a heating rate of 10 °C min^{−1}, and 10–15 mg sample mass in corundum crucibles.

3. Results and Discussion

3.1. PXRD Analysis

Powder XRD patterns of the starting and the exchanged clinoptilolite samples are presented in Figure 1. Heavy cations such as Rb^+ , Sr^{2+} , Ba^{2+} , and Cs^+ exchanged in clinoptilolite pores decreased the peak 020 markedly [42]. In our case only Cd^{2+} influenced the intensity of 020 reflection decreasing it. Intensity changes of peaks $20\bar{1}$, 001 , $3\bar{1}\bar{1}$, and 111 are observed in Mg- and Cd-exchanged clinoptilolite because these cations occupy one and the same position (M4, according [8]), preferred by smaller divalent ions. For both clinoptilolite forms peaks $20\bar{1}$ and $3\bar{1}\bar{1}$ increase their intensities while 001 and 111 reduce theirs. The peak 220 is observed only in the pattern of the monovalent K-, Na-exchanged forms and in the Natural-cpt, while the peak 310 is characteristic for bivalent Ca^{2+} - and Cd^{2+} -ones.

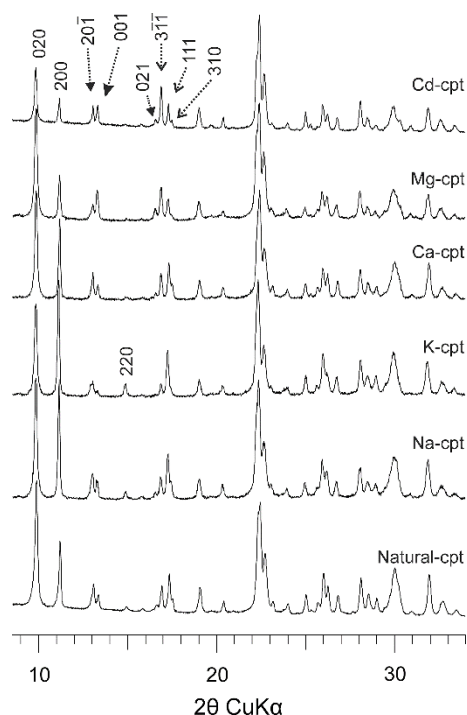


Figure 1. Powder XRD patterns of natural and ion-exchanged clinoptilolite.

3.2. EDS SEM

The performed EDS elemental analyses of the initial (purified) and exchanged clinoptilolite allowed calculations of the crystal chemical formulae of the different clinoptilolite forms (Table 1).

The chemical composition and the structural formulae of clinoptilolite are based on 72 O atoms. Among the exchanged samples predominant exchange was obtained for the Na^+ , K^+ , and Ca^{2+} forms, followed by Cd^{2+} , while the Mg^{2+} form was relatively less exchanged.

3.3. Thermal Analyses

DSC-TG (DTG) curves of natural and cation-exchanged forms of clinoptilolite from Beli Plast are presented on Figure 2. The endotherm minima temperatures are between 78 and 115 °C decreasing in the sequence $\text{K-cpt} < \text{Na-cpt} < \text{Natural-cpt} < \text{Ca-cpt} \leq \text{Mg-cpt} < \text{Cd-cpt}$ (Figure 2, Table 2). This sequence well corresponds to the size of the ionic radii of the exchangeable cations (Table 3), namely, the larger ionic radii of K^+ favors the faster dehydration of its corresponding exchanged-form compared to the others, while both the smaller ionic radii and the larger values for ionization potential of Cd^{2+} and Mg^{2+} in their respective forms affect the shift of dehydration to higher temperatures. Similar thermal

behavior has been observed by other authors in their studies of natural clinoptililite and its K-, Na-, Ca-, and Mg-exchanged forms [22,34] and Cd-modified form [23].

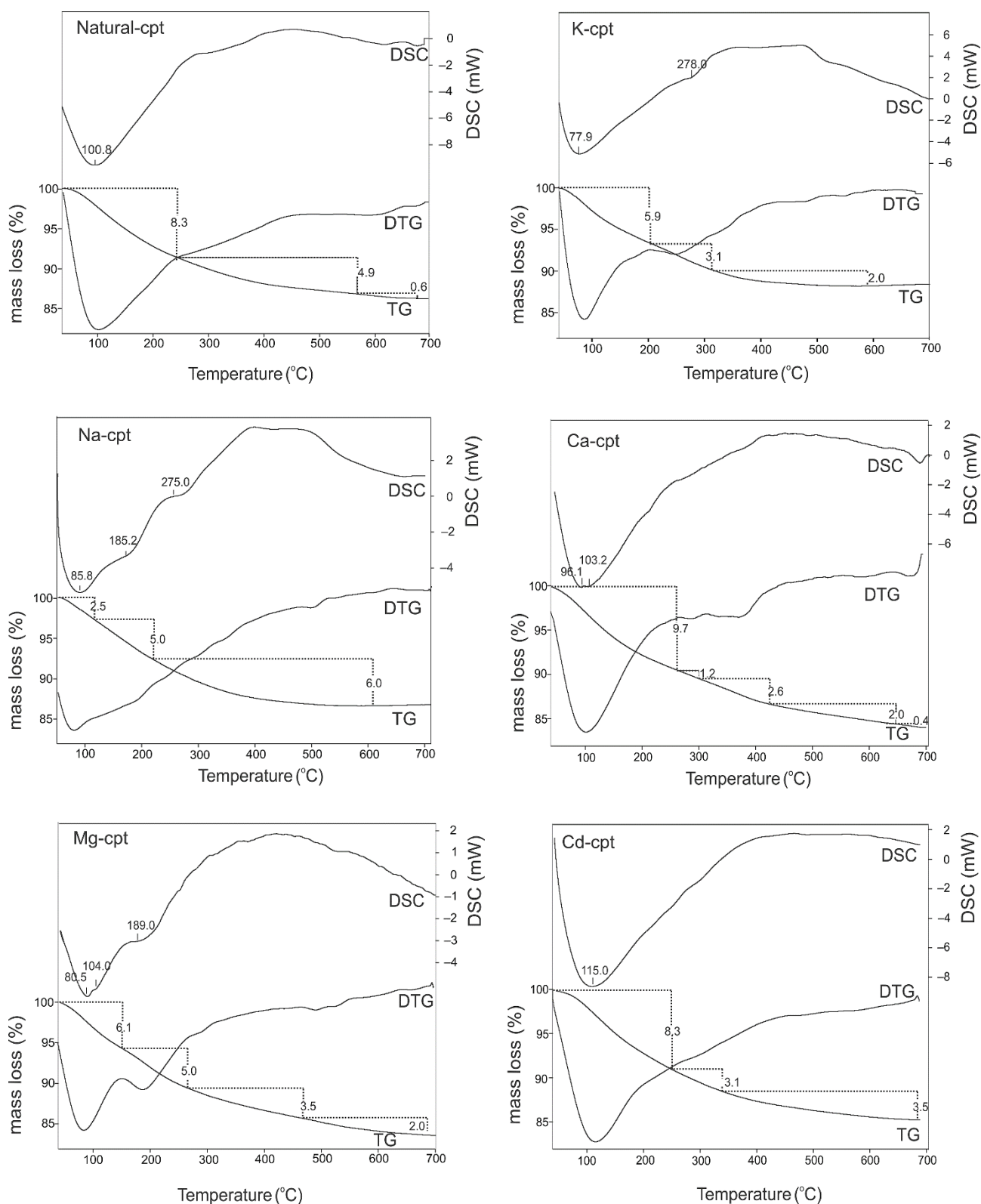


Figure 2. DSC-TG(DTG) curves of natural and exchanged forms of clinoptililite.

Table 2. Thermal analyses data of the natural and ion-exchanged forms of clinoptilolite.

Sample	Total Mass Loss, %	Total H ₂ O Molecules	Evolved H ₂ O Molecules in Low-Temperature Region	Endotherm Minima Temperature, °C
Natural-cpt	13.8	20.6	12.4 up to 230 °C	100.8
K-cpt	11.0	16.4	8.8 up to 210 °C	77.9
Na-cpt	13.3	19.6	11.0 up to 220 °C	85.8
Ca-cpt	15.5	23.3	14.5 up to 250 °C	96.1; 103.2
Mg-cpt	16.6	25.0	16.8 up to 230 °C	80.5; 104.0
Cd-cpt	14.9	23.7	13.1 up to 230 °C	115.0

Table 3. Ionic radii and ionization potentials of exchangeable cations (after Lide [43]).

Cations	Ionic Radii (Å)	Ionization Potential (eV)
K ⁺	1.37	5.13
Na ⁺	0.99	4.34
Ca ²⁺	1.00	6.11
Mg ²⁺	0.57	7.64
Cd ²⁺	0.78	8.99

The TG total mass loss data reveals decreasing of the total H₂O molecule content in the sequence K-cpt < Na-cpt < Natural-cpt < Ca-cpt < Cd-cpt < Mg-cpt which is again in agreement with the size of ionic radii of exchangeable cations and their structural hydration characteristics (Figure 2, Table 3). Some peculiarities can be noted in the TG and DTG curves of the investigated clinoptilolite samples: (i) The dehydration process is completely finished up to 500 °C for the K- and up to 600 °C for the Na-exchanged clinoptilolite, while for the bivalent cation forms of clinoptilolite this process is not completed even at 700 °C. (ii) The dehydration process is rather complicated including several stages depending on the dominant exchangeable cations: two for the initial and Cd-form, three for K- and Na-forms, and more than three for Mg- and Ca-forms. (iii) The steepest slope of the TG curves reflected in the well-defined effects on the DTG curves is observed for all samples in the temperature interval 20–300 °C. In this temperature interval the dehydration process is one-stage for the natural- and Cd-clinoptilolite and two for the K-, Na-, Ca- and Mg-forms. (iv) The natural and modified clinoptilolite structure remains stable up to 700 °C.

3.4. Rietveld Analysis

The conducted Rietveld structural analyses on the studied clinoptilolite forms converged at acceptable reliability (R) factors. Their values and the refined unit-cell parameters are given in Table 4. The quality of the fit between the calculated and observed diffraction profiles obtained in a Rietveld refinement is usually given with the standard agreement indices R_p , R_{wp} , and R_{exp} and the goodness of fit index (GoF), defined by Young [44].

The performed chemical (EDS) and XRD structural analyses show that there are residues of the initial cations (Ca²⁺, K⁺, Na⁺, and Mg²⁺) after the ion exchange procedures, which is confirmed by the refined occupancies of the cationic sites in the structure as well as by the EDS analyses (calculated as apfu). This means that in the pores of the exchanged clinoptilolites there are preserved residual cation–H₂O complexes among the dominating complexes of the incoming exchangeable cations, which influence some of the intensities of the clinoptilolite peaks (Figure 1).

It is important to note that after the structural refinements the incoming exchangeable cations predominantly occupy the positions that are typical for them in the natural clinoptilolite but do not fill these positions fully and some of them spread into other positions in the pores of the structure. One reason for this is the specific Al-distribution in the clinoptilolite framework, which controls the possible existing of potential cationic sites for best charge compensation. This results in differently configured cationic hydration shells

around one and the same cation depending on its positioning. The hydration shells of the residual and newly exchanged cations are varying and create local asymmetry on the level of the unit cell, which influences, in a different way, the thermal effects during dehydration of the samples (DSC/TG results).

Table 4. Reliability factors and unit-cell parameters of Natural-cpt and exchanged clinoptilolite forms.

	Natural-cpt	Na-cpt	Ca-cpt	K-cpt	Mg-cpt	Cd-cpt
R _{exp}	8.75	6.39	6.44	4.97	6.10	4.99
R _{wp}	7.33	9.45	8.84	6.16	9.20	6.14
R _p	6.69	7.45	6.94	4.62	7.17	4.80
GoF	1.78	1.48	1.37	1.24	1.51	1.22
R _B	3.21	2.27	2.30	1.03	2.86	1.41
a (Å)	17.6777 (8)	17.6912 (7)	17.6706 (9)	17.6838 (9)	17.6991 (7)	17.6807 (8)
b (Å)	17.9485 (1)	17.9453 (6)	17.9374 (8)	17.9898 (8)	17.9957 (8)	17.9919 (8)
c (Å)	7.4146 (4)	7.4217 (3)	7.4128 (4)	7.4151 (4)	7.4342 (3)	7.4155 (4)
β (°)	116.377 (2)	116.260 (2)	116.370 (3)	116.272 (3)	116.274 (3)	116.263 (3)
V (Å ³)	2108.4 (2)	2113.04 (2)	2105.12 (23)	2115.3 (2)	2123.22 (3)	2115.4 (3)

Note: R_{wp}—weighted profile R-factor; R_{exp}—expected R-factor; R_p—profile R-factor; GoF—goodness of fit = R_{wp}/R_{exp}; R_B—R-Bragg factor.

The XRD structural data about the positions and populations of the sites of extra-framework cations and H₂O molecules are presented in Table 5, while the values of bond distances are given in Table 6. The values marked with (*) in Table 6 are the closest distances between the cations and H₂O molecules, indicating the number of the strongly bound H₂O molecules, which leave the structure at higher temperatures (>~300 °C). The number of these H₂O molecules was subtracted from the total number of H₂O molecules calculated by TG (Table 2) for the natural and each exchanged clinoptilolite sample. In this way, the obtained values are for the non-coordinating H₂O molecules (weakly bound). According to the data from the TG analyses these molecules are released in the range from 20 °C to 200–250 °C. The comparison of the data obtained by Rietveld refinement and DSC-TG(DTG) shows similarity between these values.

Table 5. Extra-framework sites, H₂O molecules sites, and their occupancies per unit cell.

Sites	Nat-cpt	K-cpt	Na-cpt	Ca-cpt	Mg-cpt	Cd-cpt
Na1	1.01	0.22	2.79	0.32	0.32	0.28
Na2			1.82			
K1		0.39				
K2		0.68				
K3	1.11	3.17	0.35	0.24	0.41	0.36
Ca1				0.65		
Ca2	1.77	0.78	0.28	1.86	1.00	0.68
Mg	0.46	0.26	0.29	0.31	1.82	
Cd						0.80
Cd1						0.18
Cd2						0.89
Cd3						0.26
Total Cd						2.13
O11	2.08	1.66	3.21	3.02	2.51	1.52
O12	1.59	1.32	2.24	2.00	2.80	0.66
O13	7.12	5.77	5.28	6.55	4.60	4.58
O14	2	2	2	2	2	1.0
O15	2.75	1.49	2.82	1.94	2.12	1.80
O16	2.56	3.16	2.00	1.95	1.05	2.16
O17	0.09	1.64	0.24	-	1.64	2.70
O18				1.09	2.07	2.96
O19					0.72	
Total H ₂ O	18.19	17.01	17.80	18.55	19.90	16.85

Table 6. Distance between cations and H₂O molecules (values marked with (*) are the closest distances between the cations and H₂O molecules).

Samples	Cation Positions	Distance between Cations and H ₂ O Molecules Å								
		O11	O12	O13×4	O14	O15×2	O16	O17	O18	O19
Natural-cpt	Na	2.63	2.40 *			2.96	2.65			
	Ca			2.38 */2.63	2.55 *					
	K		2.93							
K-cpt	Mg					1.97 *				
	K1						2.81 *			
	K2				2.82 *					
	K3		2.94 *	3.06 *						
Na-cpt	Ca									
	Mg									
	Na1	2.62	2.40 *			2.57	2.65			
	Na2			2.43 */2.66	2.52 *					
	Ca2			2.38 */2.63	2.55 *					
Ca-cpt	K		2.93							
	Mg					1.94			2.15 *	
	Ca1	2.61	2.44 *			2.56	2.60			
	Ca2			2.39 */2.64	2.55 *					
	Na		2.48 *			2.58	2.60			
Mg-cpt	K		2.97							
	Mg					1.94			2.15 *	
	Mg		2.32 *			1.96 *		1.75	2.15 *	2.38
	Ca			2.39 */2.64	2.55 *					
Cd-cpt	Na	2.61	2.79			2.99				2.51 *
	CdM4					2.12 *	2.16 *	2.30 *		
	Cd2			2.24 *	2.06 *					
	Cd3		2.17 *					2.34 *		2.39 *
	Cd1		2.25 *			2.30 *			2.33 *	
	Ca			2.46 */2.51 *	2.72 *		2.51			

For example, in the initial natural sample, the structural refinement (Figure 3, Natural-cpt) shows five H₂O (O11, O12, O15×2, and O16) molecules around Na⁺ and another five around Ca²⁺ (O13×4 and O14) (Table 6). Around the Mg²⁺ a doubled H₂O position (O15×2) is localized at appropriate distance of 1.97 Å. The nearest H₂O molecules (up to 2.63 Å distance) around Na⁺ and Ca²⁺ positions are situated in sites O11, O12, O13, and O14. Thus, 1Na⁺, 1.77Ca²⁺, and 0.46Mg²⁺ are coordinated by about 8.2 H₂O molecules per unit cell in the porous structure. Calculations based on the data from TG analysis (Table 2) show a total of 20.6 H₂O molecules. The difference between this number and the number (8.2) of H₂O molecules near the cations (XRD data) is about 12.3. This value is very close to the number (12.4) of H₂O molecules calculated from the mass loss measured by TG analysis in the stage up to 230 °C, where both physisorbed and weakly bound water molecules are released.

In K-exchanged clinoptilolite (Figure 3, K-cpt) the K⁺ ions are localized predominantly in position K3 (corresponding to position M3—typical for clinoptilolite [8]) but also in positions K1 and K2 (Table 5). The H₂O molecules in positions O12, O13 coordinate K⁺ in position K3 and in O14 are around position K2, while K1 is coordinated by H₂O in position O16. The total number of the nearest H₂O molecules around K1, K2, and K3 positions is 8.0. The potassium-exchanged clinoptilolite shows total loss of 16.4 H₂O molecules on the TG curve (Figure 2), from which 8.8 H₂O molecules leave up to 210 °C (weakly bound). The remaining 7.6 H₂O molecules (strongly bound) are close to 8.0 H₂O from the structural study.

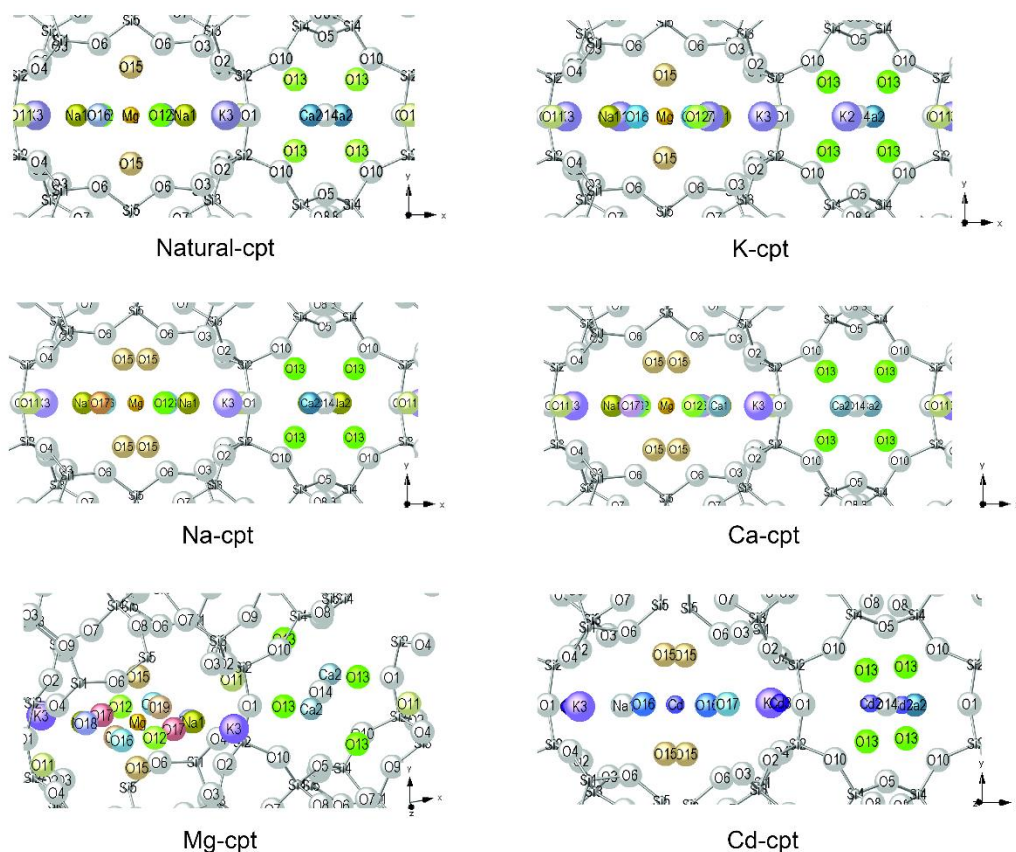


Figure 3. Structural representation of the refined cation-exchanged forms of the natural clinoptilolite.

In the structure of Na-exchanged clinoptilolite the Na^+ ions are distributed in two positions: Na1 (preferred by Na^+ in natural clinoptilolite—position M1) and Na2 (preferred by Ca^{2+} in natural clinoptilolites—position M2). The closely coordinating H_2O molecules around cationic position Na1 are concentrated in positions O11, O12, O13, O15, and O16. In the case of position Na2 the closely coordinating H_2O molecules are in O13 and O14. Based on the XRD structural results the total number of the strongly bound (up to 2.65 Å) H_2O in the above positions is 8.7. The calculations from the TG analyses give total number of 19.6 H_2O molecules (Table 2). The difference of 11.0 H_2O molecules (weakly bound and leaving the structure up to 220 °C) well corresponds to the value of 10.9 obtained by XRD structural refinement.

In the Ca-exchanged clinoptilolite, two calcium positions are structurally refined, namely Ca1 and Ca2, preferred, respectively, by sodium (in position M1) and calcium (in M2) in the natural sample (Table 5). The number of H_2O molecules closely located around these two calcium positions (in sites O11, O12, O13, O14, O15, and O16) and also around Na1 (in sites O11, O12, and O15) at a distance of up to 2.60 Å (Tables 5 and 6) is about 8.8 per unit cell. According to TG data, the calculated total number of H_2O molecules is about 23.3. The difference between the total (TG) and the closely coordinating (XRD) H_2O molecules is 14.4, which is almost equal to the calculated value of 14.5 from TG data.

In the Mg-exchanged clinoptilolite there was one refined Mg^{2+} position in the original site M4 occupied by 1.82 ions. This position is closely coordinated with H_2O positions O12, O15, and O18 occupied by 5.5 H_2O molecules (strongly bound). However, in this sample 1 Ca^{2+} was refined as residue in its original position M2 surrounded by 3 H_2O molecules in positions O13 and O14. Thus, the number of strongly bound H_2O in this sample is 8.5. The difference between 25.0 H_2O molecules (the total number of H_2O molecules calculated by TG analysis) and the 8.5 H_2O molecules around the cations (X-ray data) is 16.6 H_2O molecules, which is close to the number of weakly bound water molecules calculated by TG and released in the range up to 250 °C.

In the Cd-exchanged clinoptilolite four Cd^{2+} positions were structurally determined, namely Cd, Cd1, Cd2, and Cd3 in which the total number of refined cations is 2.13 Cd^{2+} but mostly occupied are Cd (magnesium position M4 in the original structure [8]) and Cd2 (original calcium position M2) (Table 5). The positions Cd1 and Cd3 are also occupied but in lesser amounts. The number of the nearest H_2O molecules around all cadmium positions as well as around the residual Na^+ and Ca^{2+} cations after the exchange process is 10.7. The difference between the total number of 23.7 H_2O molecules (calculated from TG data) and the number 10.7 of strongly bound H_2O (obtained by XRD structural refinement) is 13.0 H_2O molecules. Again, this value is close to the TG results for weakly bound H_2O molecules (13.1).

In all the exchanged clinoptilolite samples there remained small amounts of the original cations— Na^+ , K^+ , Ca^{2+} , Mg^{2+} found in the natural clinoptilolite. The coordinating H_2O molecules around these residues, although small in quantity exert some additional influence on the DSC-TG(DTG) curves and also it is difficult to refine them structurally by PXRD because of their low occupation of the sites.

In the performed investigations we paid attention mainly to both loosely and tightly bound water, which is an important structural fragment in clinoptilolite combined with the specific exchangeable cation arrangements, especially when we consider mono (Na^+ , K^+)- and divalent (Ca^{2+} , Mg^{2+}) ones, typical for clinoptilolite.

The calculations in our study based on DSC-TG(DTG) confirm that the total water content of the clinoptilolite forms is closely related to the content of monovalent to divalent cations. Clinoptilolites with a sum of divalent cations in the unit cell greater than 1.87 may contract after heating [1]. Higher temperatures are required to contract samples with higher Si/Al ratios, which is the case of clinoptilolite.

Our investigations confirm the dependence of the thermal behavior of clinoptilolite to its structural features (type of the exchangeable cations, their specific positioning within the structural channels, their coordination to H_2O molecules, and their interactions with framework oxygen atoms [9,10,12,32,33]). Much of the obtained data in the present study has shown that H_2O molecules in the clinoptilolite forms structurally are held with a more or less continuous range of energies, which plays an important role upon dehydration with temperature. In addition, there is a continuous rearrangement of extra-framework exchangeable cations and H_2O molecules with concomitant structural relaxation as dehydration proceeds [9,10,45]. The H_2O molecules that evolve at lower temperatures (loosely bound) are not as closely associated with the extra-framework cations and the high-energy frameworks sites as are the remaining H_2O molecules (tightly bound).

The comparison of the data obtained from Rietveld structural analyses and DSC-TG(DTG) thermal study helped to assess, which H_2O -cation bond distances are responsible for the effects in the corresponding curves: indicating weakly bound H_2O molecules up to 200–250 °C or strongly bound H_2O molecules above 250 °C.

The results for the monovalent clinoptilolite forms show fewer H_2O molecules and lesser occupation of the corresponding coordination H_2O spheres. Such forms may have application for processes at higher temperatures. In the case of bivalent cations such clinoptilolite forms possess both fewer cations and more H_2O molecules, which make them perspective for specific applications.

4. Conclusions

The crystal structural specificity and the thermal characteristics of the studied cation-exchanged clinoptilolite forms display similarities, but there are certain differences in some cases, which can be related to chemical content of the ion exchanged modifications. The performed detailed study of the dehydration specificity of natural clinoptilolite and its Na-, K-, Ca-, Mg-, and Cd-exchanged forms was based on comparative studies using DSC—TG(DTG), EDS, and Rietveld-based XRD structural analysis in order to elucidate the manner of dehydration of the H_2O molecules—loosely and tightly bound in relation to specific structural cation- H_2O configurations.

The obtained results show that the cation coordinating H₂O molecules determined by XRD structural refinement and the non-coordinating ones (given by DSC and TG(DTG) analyses) are released at different temperatures and in the thermogravimetric curves reflect the influence of the dominant exchangeable cation in the clinoptilolite structure.

Both methods are complementary in terms of elucidating the role of water in the zeolite structure—cation-coordinated H₂O is released at temperatures above 230–250 °C.

The structural position of Cd²⁺ has been clarified as it is distributed in the four cationic positions and this contributes to the similarity in thermal behavior with the natural form. The place of the Cd-form in the orders of both the hydration of the studied forms and the endotherm minima temperatures was determined.

In the case of bivalent cations (Mg²⁺, Cd²⁺, and Ca²⁺) which have higher ionization potential than the monovalent ones (Na⁺, K⁺) the total number of the H₂O molecules coordinating their sites is bigger—namely 23–25 compared to 16–20 for the monovalent cations. In addition, the larger ionic radii of K⁺ favors the faster dehydration of its corresponding exchanged-form compared to the others, while the smaller ionic radii of Cd²⁺ and Mg²⁺ in their respective forms affect the shift of dehydration to higher temperatures. As a whole, the dehydration process is completely finished up to 500 °C for the K- and up to 600 °C for the Na-exchanged clinoptilolite, while for the bivalent cation forms of clinoptilolite this process is not completed even at 700 °C.

Author Contributions: Conceptualization, L.D. and N.P.; methodology, L.D., N.P., Y.T. and O.P.; software, L.D., N.P., Y.T., O.P. and I.P.; investigation, L.D., N.P., Y.T., O.P. and I.P.; writing—original draft preparation, L.D., N.P., Y.T. and O.P.; writing—review and editing, L.D., N.P., Y.T. and O.P.; visualization, L.D., N.P. and Y.T.; funding acquisition, L.D. and Y.T. All authors have read and agreed to the published version of the manuscript.

Funding: This research was funded by Bulgarian National Science Fund, grant number KII-06-H44/3/27.11.2020.

Data Availability Statement: Not applicable.

Acknowledgments: The authors acknowledge the technical support from the project PERIMED BG05M2OP001-1.002-0005/29.03.2018 (2018–2023).

Conflicts of Interest: The authors declare no conflict of interest.

References

1. Boles, J.R. Composition, optical properties, cell dimensions, and thermal stability of some heulandite-group zeolites. *Am. Miner.* **1972**, *57*, 1463–1493.
2. Coombs, D.S.; Alberti, A.; Armbruster, T.; Artioli, G.; Colella, C.; Galli, E.; Grice, J.D.; Liebau, F.; Mandarino, J.A.; Minato, H.; et al. Recommended nomenclature for zeolite minerals: Report of the Subcommittee on Zeolites of the International Mineralogical Association, Commission on New Minerals and Mineral Names. *Can. Miner.* **1997**, *35*, 1571–1606.
3. Meier, W.M.; Olson, D.H.; Baerlocher, C. Atlas of zeolite structure types. *Zeolites* **1996**, *17*, 1–230.
4. Doebelin, N.; Armbruster, T. Stepwise dehydration and change of framework topology in Cd-exchanged heulandite. *Microporous Mesoporous Mater.* **2003**, *61*, 85–103. [[CrossRef](#)]
5. Alberti, A. The crystal structure of two clinoptilolites. *Tschermaks Miner. Petrogr. Mitt.* **1975**, *22*, 25–37. [[CrossRef](#)]
6. Carey, J.W.; Bish, D.L. Equilibrium in the clinoptilolite-H₂O system. *Am. Miner.* **1996**, *81*, 952–962. [[CrossRef](#)]
7. Merkle, A.B.; Slaughter, M. Determination and refinement of the structure of heulandite. *Am. Miner.* **1968**, *53*, 1120–1138.
8. Koyama, K.; Takeuchi, Y. Clinoptilolite: The distribution of potassium atoms and its role in thermal analysis. *Z. Kristallogr.* **1977**, *145*, 216–239. [[CrossRef](#)]
9. Armbruster, T.; Gunter, M.E. Stepwise dehydration of heulandite-clinoptilolite from Succor Creek Oregon, U.S.A.: A single-crystal X-ray study at 100 K. *Am. Miner.* **1991**, *76*, 1872–1883.
10. Armbruster, T. Dehydration mechanism of clinoptilolite and heulandite; single-crystal X-ray study of Na-poor, Ca-, K-, Mg-rich clinoptilolite at 100 K. *Am. Miner.* **1993**, *78*, 260–264.
11. Cappelletti, P.; Langella, A.; Cruciani, G. Crystalchemistry and synchrotron Rietveld refinement of two different clinoptilolites from volcanoclastites of Northwestern Sardinia. *Eur. J. Miner.* **1999**, *11*, 1051–1060. [[CrossRef](#)]
12. Bish, D.L.; Carey, J.W. Thermal behavior of natural zeolites. In *Natural Zeolites: Occurrence, Properties, Applications (Reviews in Mineralogy and Geochemistry)*; Bish, D.L., Ming, D.W., Eds.; Mineralogical Society of America: Washington, DC, USA, 2001; Volume 45, pp. 403–452.

13. Mumpton, F.A. Clinoptilolite redefined. *Am. Miner.* **1960**, *45*, 351–369.
14. Mason, B.; Sand, L.B. Clinoptilolite from Patagonia: The relationship between clinoptilolite and heulandite. *Am. Miner.* **1960**, *45*, 341–350.
15. Akdeniz, Y.; Ülkü, S. Thermal stability of Ag-exchanged clinoptilolite rich mineral. *J. Therm. Anal. Calorim.* **2008**, *94*, 703–710. [[CrossRef](#)]
16. Alberti, A. The structure type of heulandite B (heat-collapsed phase). *Tschermaks Miner. Petrogr. Mitt.* **1973**, *19*, 173–184. [[CrossRef](#)]
17. Alberti, A.; Vezzalini, G. The thermal behaviour of heulandites: A structural study of the dehydration of Nadap heulandite. *Tschermaks Miner. Petrogr. Mitt.* **1983**, *31*, 259–270. [[CrossRef](#)]
18. Galli, E.; Gottardi, G.; Mayer, H.; Preisinger, A.; Passaglia, E. The structure of potassium-exchanged heulandite at 293, 373 and 593 K. *Acta Crystallogr.* **1983**, *B39*, 189–197. [[CrossRef](#)]
19. Knowlton, G.D.; White, T.R.; McKague, H.L. Thermal study of types of water associated with clinoptilolite. *Clays Clay Miner.* **1981**, *29*, 403–411. [[CrossRef](#)]
20. Duvarci, Ö.Ç.; Akdeniz, Y.; Özmuş, F.; Ülkü, S.; Balköse, D.; Çiftçi, M. Thermal behaviour of a zeolitic tuff. *Ceram. Int.* **2007**, *33*, 795–801. [[CrossRef](#)]
21. Chmielewska, E.; Sabová, L.; Jesenák, K. Study of adsorption phenomena ongoing onto clinoptilolite with the immobilized interfaces. *J. Therm. Anal. Calorim.* **2008**, *92*, 567–571. [[CrossRef](#)]
22. Alver, B.E.; Sakizci, M.; Yörükoğullari, E. Investigation of clinoptilolite rich natural zeolites from Turkey: A combined XRF, TG/DTG, DTA and DSC study. *J. Therm. Anal. Calorim.* **2010**, *100*, 19–26. [[CrossRef](#)]
23. Ünal, T.; Mızrak, İ.; Kadir, S. Physicochemical characterisation of natural K-clinoptilolite and heavy-metal forms from Gördes (Manisa, western Turkey). *J. Mol. Struct.* **2013**, *1054*, 349–358. [[CrossRef](#)]
24. Zvereva, I.A.; Shelyapina, M.G.; Chislov, M.; Novakowski, V.; Malygina, E.; Rodríguez-Iznaga, I.; Hernández, M.-A.; Petranovskii, V. A comparative analysis of natural zeolites from various Cuban and Mexican deposits: Structure, composition, thermal properties and hierarchical porosity. *J. Therm. Anal. Calorim.* **2022**, *147*, 6147–6159. [[CrossRef](#)]
25. Alietti, A. Polymorphism and crystal-chemistry of heulandites and clinoptilolites. *Am. Miner.* **1972**, *57*, 1448–1462.
26. Alietti, A.; Gottardi, G.; Poppi, L. The heat behavior of the cation exchanged zeolites with heulandite structure. *Tschermaks Miner. Petrogr. Mitt.* **1974**, *21*, 291–298. [[CrossRef](#)]
27. Tsolis-Katagas, P.; Katagas, C. Zeolitic diagenesis of Oligocene pyroclastic rocks of the Metaxades area, Thrace, Greece. *Miner. Mag.* **1990**, *54*, 95–103. [[CrossRef](#)]
28. Kitsopoulos, K.P. The relationship between the thermal behavior of clinoptilolite and its chemical composition. *Clays Clay Miner.* **2001**, *49*, 236–243. [[CrossRef](#)]
29. Kantiranis, N.; Chrissafis, C.; Filippidis, A.; Paraskevopoulos, K.M. Thermal distinction of HEU-type mineral phases contained in Greek zeolite-rich volcanoclastic tuffs. *Eur. J. Miner.* **2006**, *18*, 509–516. [[CrossRef](#)]
30. Kudoh, Y.; Takeuchi, Y. Thermal stability of clinoptilolite: The crystal structure at 350 °C. *Miner. J.* **1983**, *11*, 392–406. [[CrossRef](#)]
31. Christidis, G.E.; Moraetis, D.; Keheyan, E.; Akhalbedashvili, L.; Kekelidze, N.; Gevorkyan, R.; Yeritsyan, H.; Sargsyan, H. Chemical and thermal modification of natural HEU-type zeolitic materials from Armenia, Georgia and Greece. *Appl. Clay Sci.* **2003**, *24*, 79–91. [[CrossRef](#)]
32. Bish, D.L. Effects of exchangeable cation composition on the thermal expansion/contraction of clinoptilolite. *Clays Clay Miner.* **1984**, *32*, 444–452. [[CrossRef](#)]
33. Bish, D.L. Thermal behavior of natural zeolites. In *Natural Zeolites '93: Occurrence, Properties, Use*; Ming, D.W., Mumpton, F.A., Eds.; Brockport: New York, NY, USA, 1993; pp. 259–269.
34. Langella, A.; Pansini, M.; Cerri, G.; Cappelletti, P.; De' Gennaro, M. Thermal behavior of natural and cation-exchanged clinoptilolite from Sardinia (Italy). *Clays Clay Miner.* **2003**, *51*, 625–633. [[CrossRef](#)]
35. Cruciani, G. Zeolites upon heating: Factors governing their thermal stability and structural changes. *J. Phys. Chem. Solids* **2006**, *67*, 1973–1994. [[CrossRef](#)]
36. Aleksiev, B.; Djourova, E.G. On the origin of zeolite rocks. *Comptes. Rendus. Acad. Bulg. Sci.* **1975**, *28*, 517–520.
37. Yanev, Y.; Cocheme, J.-J.; Ivanova, R.; Grauby, O.; Burlet, E.; Pravchanska, R. Zeolites and zeolitization of acid pyroclastic rocks from paroxysmal Paleogene volcanism, Eastern Rhodopes, Bulgaria. *Neues Jahrb. Miner. Abh.* **2006**, *182*, 265–283. [[CrossRef](#)]
38. Yanev, Y.; Ivanova, R. Post-Conference Field Trip Guidebook Eastern Rhodopes, South Bulgaria. In *Proceedings of the Zeolite 2010—8th International Conference of the Occurrence, Properties, and Utilization of Natural Zeolites*, Sofia, Bulgaria, 10–18 July 2010; p. 34.
39. Dimowa, L.T.; Petrov, O.E.; Djourelou, N.I.; Shivachev, B.L. Structural study of Zn-exchanged natural clinoptilolite using powder XRD and positron annihilation data. *Clay Miner.* **2015**, *50*, 41–54. [[CrossRef](#)]
40. Rietveld, H.M. A profile refinement method for nuclear and magnetic structures. *J. Appl. Crystallogr.* **1969**, *2*, 65–71. [[CrossRef](#)]
41. *Topas V4.2: General Profile and Structure Analysis Software for Powder Diffraction*; Bruker AXS: Karlsruhe, Germany, 2009.
42. Petrov, O.E. Cation exchange in clinoptilolite: An X-ray powder diffraction analysis. In *Natural Zeolites '93 Occurrence, Properties, Use*; Ming, D.W., Mumpton, F.A., Eds.; ICNZ: Brockport, NY, USA, 1995; pp. 271–279.
43. Lide, D.R. (Ed.) *CRC Handbook of Chemistry and Physics*; CRC Press: New York, NY, USA, 2003; Volume 84.

-
44. Young, R.A. Introduction to the Rietveld Method. In *The Rietveld Method*; International Union of Crystallography, Monographs in Crystallography; Young, R.A., Ed.; Oxford University Press: New York, NY, USA, 1993; pp. 1–38.
 45. Bish, D.L. Effects of composition on the dehydration behavior of clinoptilolite and heulandite. In *Occurrence, Properties and Utilization of Natural Zeolites*; Kalló, D., Sherry, H.S., Eds.; Akademiai Kiado: Budapest, Hungary, 1988; pp. 565–576.